

## Progress towards Steady State at Low Aspect Ratio on the National Spherical Torus Experiment (NSTX)

D. A. Gates<sup>1</sup>, J. Menard<sup>1</sup>, R. Maingi<sup>2</sup>, S. Kaye<sup>1</sup>, S.A. Sabbagh<sup>3</sup>, S. Diem<sup>1</sup>, J.R. Wilson<sup>1</sup>, M.G. Bell<sup>1</sup>, R.E. Bell<sup>1</sup>, J. Ferron<sup>4</sup>, E.D. Fredrickson<sup>1</sup>, C.E. Kessel<sup>1</sup>, B.P. LeBlanc<sup>1</sup>, F. Levinton<sup>5</sup>, D. Mueller<sup>1</sup>, R. Raman<sup>6</sup>, T. Stevenson<sup>1</sup>, D. Stutman<sup>7</sup>, G. Taylor<sup>1</sup>, K. Tritz<sup>7</sup>, H. Yu<sup>5</sup>, and the NSTX Research Team

<sup>1</sup>Princeton Plasma Physics Laboratory, Princeton University, Princeton, NJ, USA

<sup>2</sup>Oak Ridge National Laboratory, Oak Ridge, TN, USA

<sup>3</sup>Dept. of Applied Physics, Columbia Univ., NYC, NY, USA

<sup>4</sup>General Atomics, San Diego, CA, USA

<sup>5</sup>Nova Photonics, Princeton, NJ, USA

<sup>6</sup>University of Washington, Seattle, WA, USA

<sup>7</sup>Johns Hopkins University, Baltimore, MD, USA

**Abstract.** Modifications to the plasma control capabilities and poloidal field coils of NSTX have enabled a significant enhancement in shaping capability which has led to the achievement of a record shape factor ( $S \equiv q_{95}(I_p/aB_t)$ ) of  $\sim 41[MA/m \cdot Tesla]$  simultaneous with a record plasma elongation of  $\kappa \equiv b/a \sim 3$ . This result was obtained using isoflux control and real-time equilibrium reconstruction. Achieving high shape factor is an important result for future ST burning plasma experiments as exemplified by studies for future ST reactor concepts, as well as neutron producing devices, which rely on achieving high shape factors in order to achieve steady-state operation while maintaining MHD stability. Statistical evidence is presented that demonstrates the expected correlation between increased shaping and improved plasma performance. Plasmas with high shape factor have been sustained for pulse lengths which correspond to  $\tau_{pulse} = 1.6s \sim 50\tau_E \sim 5\tau_{CR}$ , where  $\tau_{CR}$  is the current relaxation time and  $\tau_E$  is the energy confinement time. Plasmas with higher  $\beta_t \sim 20\%$  have been sustained for  $\tau_{pulse} = 1.2s \sim 25\tau_E \sim 3\tau_{CR}$  with non-inductive current fractions  $f_{NI} \sim 50\%$ , with  $\sim 40\%$  pressure driven current and  $\sim 10\%$  neutral beam driven current. An interesting feature of these discharges is the observation that the central value of the safety factor  $q(0)$  remains elevated and constant for several current diffusion times, similar to the “hybrid mode”. Calculations of the profiles of inductive and non-inductive current are compared to measurements of the total current profile and are shown to be in quantitative agreement. Results are shown from experiments which investigate the applicability of High Harmonic Fast Waves and Electron Bernstein Waves as current drive and heating sources, and the possibility of LHCD for future ST devices is raised. A calculated scenario which provides 100% non-inductive current drive is described. NSTX operates with peak divertor heat fluxes which are in the same range as those expected for the ITER device, i.e. with  $P_{heat_{max}} \sim 10MW/m^2$ . High triangularity, high elongation plasmas on NSTX have been demonstrated to have reduced peak heat flux to the divertor plates to  $< 3MW/m^2$ .

### 1. Introduction

The spherical torus (ST) concept [1] has been proposed as a potential fusion reactor [2] as well as a Component Test Facility (CTF) [3]. The National Spherical Torus Experiment (NSTX) was designed [4] to develop understanding of the fundamental physics issues which need to be addressed before these forward looking designs can be realized. In particular, one of the fundamental differences between low aspect ratio and standard aspect ratio tokamaks is the relatively small space available in the central conductor for a neutron shield at low aspect ratio. In order to provide sufficient shielding to incorporate super-conducting toroidal field magnets, standard aspect ratio tokamaks employ a neutron shield of order 1m in thickness. This is required to reduce the nuclear heating of the super-conducting coil to acceptable values. The central conductor of low aspect-ratio devices

typically have radii less than 1m. For this reason, the toroidal field (TF) conductor in an ST burning plasma device is usually imagined to be made of normally conducting material. Minimization of the recirculating power from this normally conducting TF coil in turn determines the minimum allowable ratio of plasma pressure to toroidal field energy  $\beta_t \equiv 2\mu_0\langle P\rangle/B_t^2$  where  $\langle P\rangle$  is the volume averaged pressure and  $B_t$  is the toroidal field at the plasma geometric center.

Additionally, it is very difficult to envision a multi-turn transformer coil that can survive in this high neutron flux environment. Therefore, it is paramount to maximize the bootstrap current and to incorporate efficient non-inductive current drive schemes at low aspect ratio, so as to reduce the external current drive power requirements. Optimizing the bootstrap current forces operation at high values of the ratio of plasma pressure to poloidal magnetic field  $\beta_p \equiv 2\mu_0\langle P\rangle/\langle B_p\rangle^2$  where  $\langle P\rangle$  is the volume averaged pressure and  $\langle B_p\rangle$  is the average poloidal field in the plasma, since  $f_{bs} \sim \sqrt{\epsilon}\beta_p$ , where  $f_{bs}$  is the bootstrap fraction,  $\epsilon \equiv 1/A \equiv a/R$ , with  $a$  and  $R$  the plasma minor and major radii, respectively.

Since the maximum pressure in the plasma is determined by the Troyon-limit given by  $\beta_N < C_T$  where  $\beta_N \equiv \beta_t a B_t / I_p$  with  $I_p$  the plasma current, the simultaneous requirements of high  $\beta_p$  and high  $\beta_t$  are at odds with each other. Raising the plasma current serves to raise the attainable  $\beta_t$ , but simultaneously reduces  $\beta_p$  (by increasing the  $\langle B_p\rangle$ ). This conflict is the motivation for attaining high plasma shaping in toroidal confinement devices. It allows for the improvement of both parameters of interest in a steady state tokamak,  $\beta_t$  and  $f_{bs}$ . It also motivates the definition of a performance parameter  $f_{bs}\beta_t \sim S\beta_N^2$  [5] where  $S \equiv q_{95}(I_p/aB_t)$  is the plasma shaping factor. The parameter  $f_{bs}\beta_t$  has been called the sustained  $\beta$ ,  $\beta_{sus}$  [6].

## 2. Improvements in Plasma Shaping Capability on NSTX

The ability to make plasmas with high elongation was shown on NSTX in 2004 [7, 8]. Stability calculations indicated that much stronger shaping was advantageous on NSTX and achievable by increasing the triangularity in concert with the elongation. Triangularity has a much stronger effect on the shape factor,  $S$ , at low aspect ratio than it does at high aspect ratio [9]. In order to achieve the desired improvements in machine shaping capability, modifications were made to the poloidal field coils on NSTX. In particular, the PF1A shaping coil shown in Figure 1 was reduced in height, while roughly preserving its total current capability, to allow for the simultaneous achievement of high elongation and high triangularity.

Along with the poloidal field coil modifications, the NSTX plasma control system [10] has been upgraded [11] to support the expanded requirements for plasma shape control. In particular, precise rtEFIT/isoflux [12, 13] control of the plasma boundary during the current ramp-up phase at high elongation required the addition of magnetic field sensors in the divertor region and a more accurate vessel current model [14] with additional measurement constraints. Although not the subject of this paper, the control system was

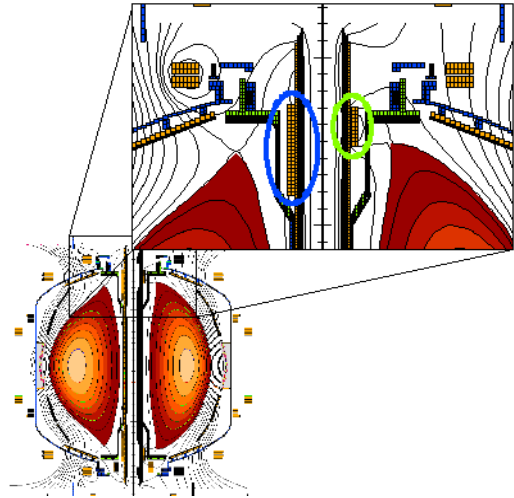


Figure 1: Detail view of the change made to the PF1A coil. The old coil is shown circled on the left, the new coil on the right.

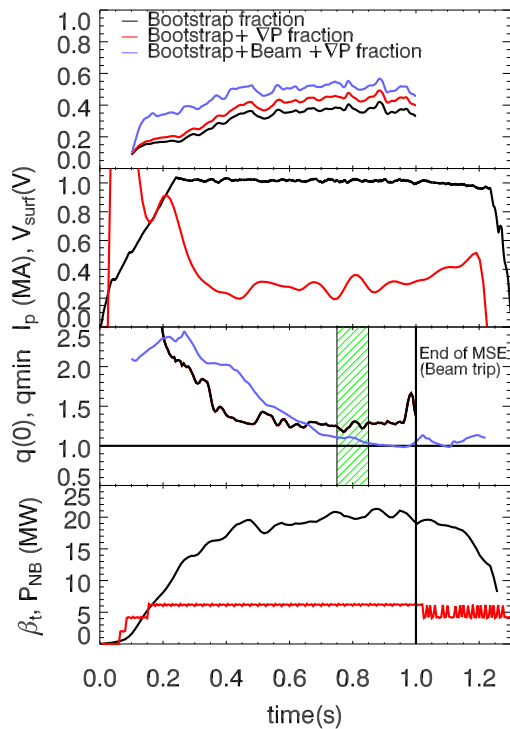


Figure 2: The time history of shot 120001 showing a) the components of non-inductive current as indicated in the plot legend, b) the plasma current (black) and the surface voltage (red), c) the reconstructed  $q(0)$  (black) and  $q_{min}$  (red) and  $q(0)$  as determined by a TRANSP magnetic diffusion calculation (blue), and d)  $\beta_t$  (black) and the neutral beam power (red). The profiles in Figure 5 are calculated over time interval indicated in green.

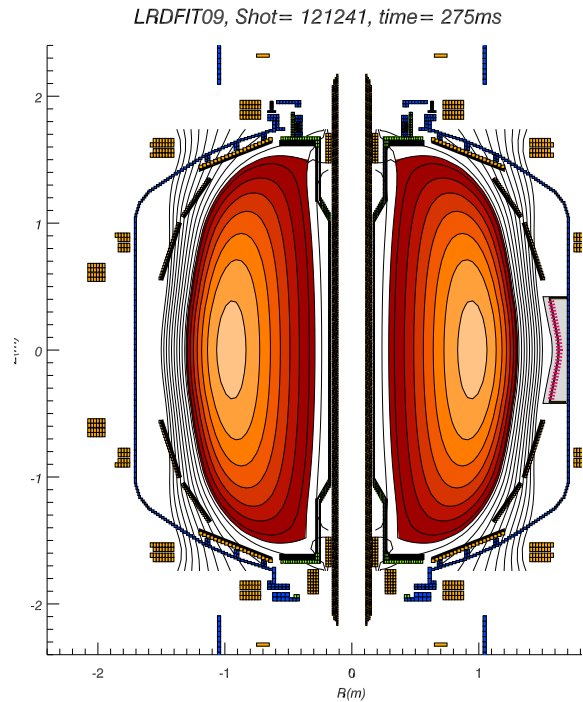


Figure 3: Flux plot of the record elongation plasma equilibrium.

also expanded to include capabilities for resistive wall mode feedback experiments [15] and error field control experiments [16].

### 3. Shape Control and Global Performance

During the 2005 campaign rtEFIT was commissioned with the expanded control system and was used to control plasmas in steady state. During the 2006 campaign, the target equilibrium identified during the design process for the specified upgrades was achieved and maintained for long pulse. The time history of an example shot with strong shaping ( $\kappa(\equiv b/a) \sim 2.4$ ,  $\delta \sim 0.8$ ) is shown in Figure 2. The calculated fraction of non-inductive current in this discharge is  $\sim 50\%$

Additional experiments have led to the achievement of a record value of the plasma shaping parameter  $S \equiv q_{95}I_p/(aB_t)$ , simultaneous with the achievement of record elongation,  $\kappa = 3$ . The previous record controlled value of plasma elongation,  $\kappa \sim 2.8$  was achieved on TCV [17]. Higher values of elongation have been reported in transient plasmas on the START device [18], but these were uncontrolled. For this discharge,  $\kappa > 2.8$  for 40ms which is  $\sim 3\tau_{vert}$ , where  $\tau_{vert}$  is the growth time for the  $n = 0, m = 1$  (vertical) plasma mode. A flux plot of the record  $\kappa$  equilibrium is shown in Figure 3.

The predicted improvement in performance as a function of increased plasma shaping is confirmed in Figure 4. Each point in this figure represents the value of  $\beta_t$  time averaged over the  $I_p$  flat-top plotted versus the flat-top time. The data are sorted in two different ways: in the lower frame by shape factor,  $S$ , and in the upper frame by year. As can be seen from the figure, the increasing shape factor on NSTX has led to an increase in both the maximum pulse length and the average value of  $\beta_t$ . The shapes of the upper boundaries in this plot are a direct result of the relationship  $f_{bs}\beta_t \sim S\beta_n^2$ . For a given  $S$ , the upper bound of the operating space is determined by  $\beta_n = \beta_{N(max)}$ , so for higher  $\beta_t$  one has lower  $f_{bs}$  yielding a shorter pulse. Increasing  $S$  acts as a multiplier on this curve. This is true in any device, such as NSTX, wherein the available transformer flux limits the pulse length (as is eventually the case for all devices that employ ohmic current drive).

#### 4. Current Profile Analysis

It is important to demonstrate the utility of models which are routinely used to calculate the magnitude and the profiles of non-inductive current. This establishes the confidence with which one can make quantitative predictions regarding the performance of future devices. It also verifies the applicability of these models at low aspect ratio, expanding the parameter space over which the models have been bench-marked against experiment. In order to make a valid comparison to data, an accurate measurement of the plasmas internal field distribution is required. The Motional Stark Effect diagnostic on NSTX, which measures the magnetic field pitch angle at 12 spatial channels, is the only such measurement currently available for any ST. This capability has been used to make a quantitative comparison between the measured and expected plasma current profiles.

Shown in Figure 5 are the total plasma current profile as determined by the MSE measurement and reconstructed by the LRDFIT equilibrium reconstruction code. Also plotted in the figure is: 1) the neutral beam driven current as calculated by the TRANSP code [19], 2) the neoclassical pressure driven currents according to a recent calculation that includes corrections important at low aspect ratio [20], and 3) the inductively driven current calculated according to the inferred time varying toroidal electric field as calculated by taking the time derivative of the flux from the equilibrium reconstructions multiplied by the calculated neoclassical resistivity. The neoclassical resistivity is also taken from reference [20]. The reconstruction process and data analysis that goes into this detailed profile comparison are described in detail in [21]. All parameters in the predicted profiles are measured ( $n_e, T_e$ , [from Thomson scattering]  $T_i, n_i, Z_{eff}$ , [from Charge Exchange Recombination Spectroscopy] and  $J_{||}$  [from Motional Stark Effect Polarimetry and external magnetics]) except the fast ion pressure profile which is calculated according to

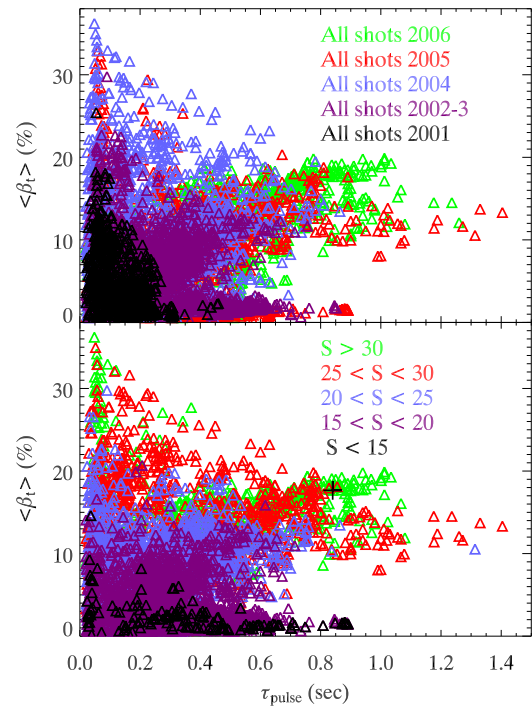


Figure 4:  $\beta_t$  averaged over the plasma current flat-top for each shot in the NSTX database plotted vs. the current flat-top time. The data is sorted according to year in the upper frame, and according to shape factor  $S$  in the lower frame.

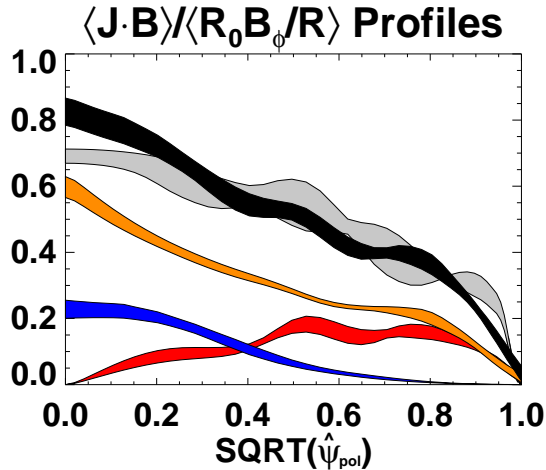


Figure 5: Components of the total current profile plotted versus flux label for shot 120001. The bootstrap current is in red, the ohmic current is in orange, and the beam driven current is in blue. The bands are variations during the time window for the calculation. The black trace is the total predicted current, and the gray is the total current as determined by equilibrium reconstruction with MSE.

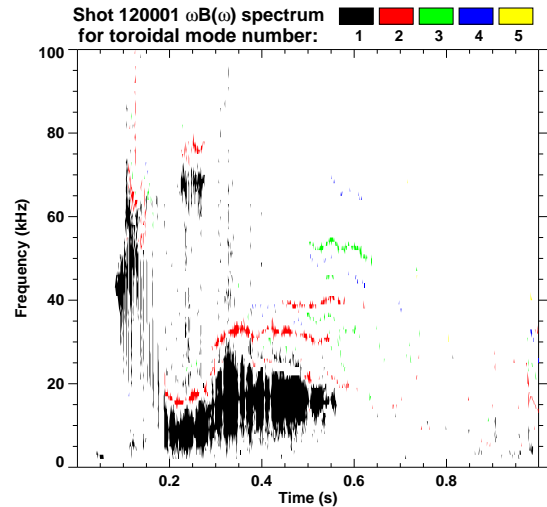


Figure 6: A spectrogram of magnetic fluctuations as measured by a Mirnov coil for shot 120001. The colors represent toroidal mode numbers as indicated in the legend. Notice the period of time after 0.6s where there are only small amplitude high- $n$  MHD modes present.

classical slowing down theory in TRANSP. This particular discharge has a non-inductive current fraction of  $f_{NI} \sim 50\%$ , less than the maximum values of  $f_{NI} \sim 65\%$  reported previously in reference [6], but has higher  $\beta_t \sim 20\%$  similar to the values typical of CTF. The pressure-driven current fraction is  $f_{pres} \sim 40\%$ , also very close to values required for CTF (typically  $\sim 50\%$ ). This discharge has  $f_{bs}\beta_t \sim 7\%$ , which is a record value. In CTF, the neutral-beam driven current fraction  $f_{NB} \sim 50\%$  is expected to be much higher, due to the expected lower collisionality at higher  $B_t$ . The profile of the total parallel current inferred from MSE measurements shown in 5 should be compared directly to the sum of the predicted parallel currents. The agreement between predicted and measured is quite good with a maximum discrepancy of  $\sim 10\%$ . The profiles do vary somewhat in the core of the discharge, which may be due to a mechanism similar to that discussed in reference [21]. The central safety factor, which is shown in Figure 2 stays elevated for  $\sim 2\tau_{CR}$  [22], similar to the “hybrid mode” proposed for ITER. For this discharge however, there is no clear evidence of a large scale MHD instability to drive fast particle diffusion. The only measured MHD modes have relatively high toroidal mode numbers  $n = 3 - 5$  during most of the period of elevated central  $q$ . A spectrogram of the measured magnetic fluctuations for the same plasma discharge presented in Figure 2 is shown in the Figure 6. Work is ongoing into what is responsible for the maintenance of the elevated central safety factor. The clear advantage of this regime of operation, which has a confinement enhancement factor of  $H89P \sim 2$ , is that the observed mode activity does not degrade confinement.

## 5. RF Heating and Current Drive

The Electron Bernstein Wave (EBW) is especially attractive since it has been shown theoretically to have very high efficiency Ohkawa type current drive. Research into the coupling of the EBW out of the plasma has indicated that the B-X-O mode conversion scheme can have efficiencies as high as 80-90%. This is encouraging, since the EBW is an



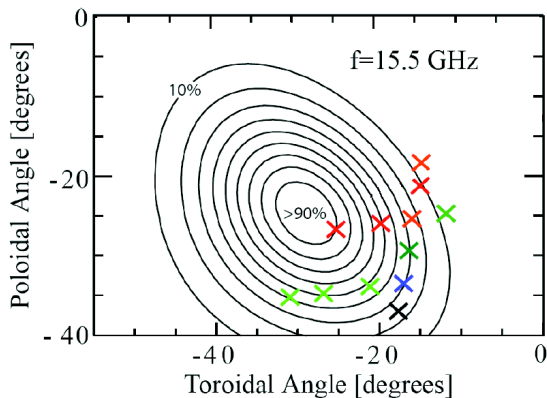


Figure 7: Data on efficiency of EBW emission from identical plasmas for which the EBW antenna pointing angle is varied. The colors represent efficiencies of 81-90% (red), 71-80% (orange), 61-70% (green), 51-60% (blue), 41-50% (purple), 31-40% (black). The ellipses are contours of theoretically predicted emission efficiency

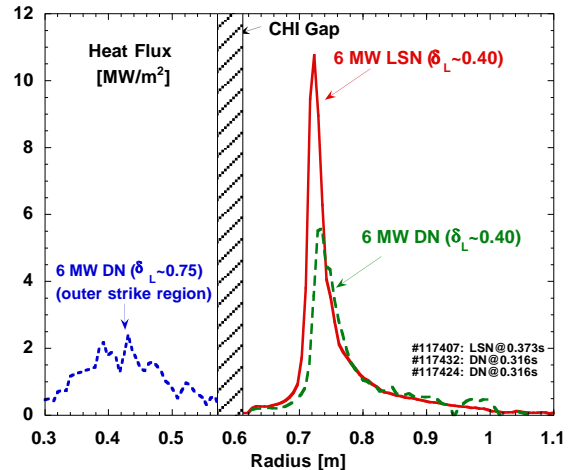


Figure 8: The peak heat flux versus major radius for three divertor configurations: 1) low  $\delta$  lower single null, 2) low  $\delta$  double null, and 3) high  $\delta$  double null. All three configurations had identical heating power. The peak heat flux reduces by a factor of  $\sim 5$ .

electrostatic wave that is evanescent in the plasma boundary, an efficient mode coupling scheme is required in order to launch high power electromagnetic waves that can transfer their energy to the plasma. Results of an experiment to investigate the angular variation of the emission efficiency are shown in Figure 7 and show good agreement with theoretical predictions. This experiment is described in more detail in [24]. The good coupling results to date have been observed in the L-mode, with much lower efficiencies of  $\sim 30\%$  in the H-mode.

Research into the use of High Harmonic Fast Wave (HHFW) heating on NSTX has for the first time yielded high efficiency coupling using the current-drive phasing ( $k_{\parallel} = 7m^{-1}$ ) of the NSTX HHFW antenna. The improved coupling was observed at higher values of toroidal field  $B_t = 0.55T$ . The higher field is thought to have reduced the parasitic coupling of the launched RF power to the parametric decay instability, which had been observed to interfere with the coupling at lower toroidal field [23]. This is an important step towards using the HHFW as a tool for driving current during the start-up phase of the NSTX plasma to aid plasma current ramp-up. The HHFW experiments are described in more detail in reference [16]

Another encouraging prediction [25] is that in future ST devices operating at higher plasma density and toroidal field it may be possible to drive current using Lower Hybrid Current Drive (LHCD). LHCD has the distinct advantage of being a widely demonstrated and effective current drive scheme. The calculations indicate that wave accessibility, as determined by the expression:

$$n_{\parallel crit} = \frac{\omega_{pe}}{\omega_{ce}} + \sqrt{1 + \frac{\omega_{pi}^2}{\omega^2} \left( \frac{\omega^2}{\omega_{ce}\omega_{ci}} - 1 \right)}$$

is achievable in a CTF like device with parameters of  $B_t \sim 2T$ ,  $n_e \sim 1.0 \times 10^{20}m^{-3}$  and a frequency of  $f \sim 5GHz$  as long as  $n_{\parallel} \gtrsim 3$ . Additionally, one can calculate that the damping of the wave is possible for waves of this scale for electron temperatures  $T_e \sim 4keV$ . Current drive efficiencies are estimated to be in the range  $\eta \sim 0.1 - 0.2A/W$ .

Larger ST devices may therefore have a simpler time driving current than do present ST experiments.

## 6. Divertor Power Loading

Controlling peak heat flux is a critical issue for ITER and other burning plasma experiments, including potential future ST experiments. An additional benefit of strong shaping, and in particular high triangularity, at low aspect ratio is strong divertor flux expansion. In lower flux-expansion regimes, the divertor power loading on NSTX is similar to that expected for ITER as first shown in Reference [26]. Figure 8 shows the effect of varying plasma shape on divertor power loading. Each shot in the figure has identical heating power, but by changing from low triangularity  $\delta \sim 0.4$  single-null to low triangularity double-null to high triangularity  $\delta \sim 0.8$  double-null, the peak heat flux is successively reduced from  $\sim 10\text{MW/m}^2$  to  $\sim 5\text{MW/m}^2$  to  $\sim 2.5\text{MW/m}^2$ . The ability to study heat flows in varying divertor geometries is a powerful tool for understanding the impact of high heat flux on plasma facing materials. In addition, the ability to raise the divertor power load to ITER-like levels in NSTX provides an excellent opportunity to qualify differing divertor technologies in a smaller, and hence less costly environment. An additional benefit of the high  $\delta$  double-null configuration is that it is consistent with operating in a small-ELM regime, first described in Reference [27].

## 7. Projections to 100% non-inductive Current Drive

Using the current drive prediction methods described in section 5, self-consistent scenarios have been identified by which NSTX can attain 100% non-inductive current drive using only bootstrap current and neutral beam current drive. The profiles of non-inductive current for one such scenario are shown in Figure 9. The bulk of the current in this case is bootstrap current, and the plasma has high  $\beta_p \sim 2.7$ . The required shaping for this scenario,  $\kappa \sim 2.6$ ,  $\delta \sim 0.8$  has already been achieved. However, in order to achieve the goal of 100% non-inductive operation, it will first be necessary to raise the electron temperature and also lower the electron density beyond that which has been typically achieved, in order to reduce the collisionality. The required increase in electron temperature is on the order of 50% for the scenario described in Figure 9. Reduction in collisionality affects not only the neutral beam driven current but also the bootstrap current in the regime that NSTX currently operates. The regime of operation that is required to achieve full non-inductive current drive in NSTX is different than that anticipated on a CTF-like device due to the lower electron temperatures achievable at the NSTX toroidal field. For a CTF like device, it is anticipated that the lower collisionality will make NBICD much more efficient, and that 100% non-inductive operation will be achievable with 50% NBICD and 50% bootstrap fraction.

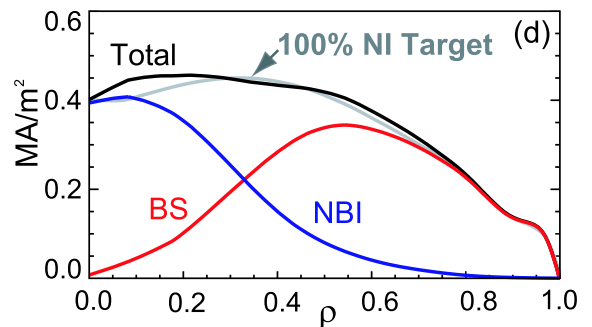


Figure 9: Calculated current profiles for a 100% non-inductively driven scenario predicted for NSTX. Successful realization of this scenario depends on reducing collisionality.

Efforts are underway on NSTX to increase the electron temperature by controlling recycling through lithium coating. This technique has already been used to successfully raise temperatures and reduce wall fueling [28].

## 8. Summary and Conclusions

NSTX has demonstrated significant progress in plasma shape control capability as evidenced by the simultaneous achievement of record plasma shaping factor  $S = 41(MA/(m \cdot Tesla))$  and  $\kappa = 3$ . These goals were achieved as a result of machine and control system improvements that have taken place over the last three years. The improved shaping capability has broadened the NSTX operating space to include plasmas with  $f_{NI} \sim 50\%$  simultaneous with  $\beta_t \sim 20\%$ . Theoretical predictions of the total current profile based on the actual measured kinetic profiles are in excellent agreement (to an accuracy  $\sim 10\%$ ), with the total measured current. This predictive capability gives increased confidence in the ability to project current-drive requirements for future devices. Several promising RF current drive options are being investigated including HHFW, EBW and the possibility of LHCD in future devices. However, 100% non-inductive operational scenarios have been identified using NBICD and bootstrap current alone. Future work on NSTX will focus on reducing the electron collisionality via edge recycling control. These results are promising for the ST concept as a future component test facility, and as a future fusion reactor device.

This work was supported by the U.S. Department of Energy Grant under contract number DE-AC02-76CH03073.

## References

- [1] Y-K. M. Peng and D. J. Strickler, Nucl. Fusion **26**, (1986) 769
- [2] F. Najmabadi and the ARIES Team, Fusion Engineering and Design, **65** (2003) 143
- [3] Y.- K M. Peng, P. J. Fogarty, T. W. Burgess, *et al.*, Plasma Physics Controll. Fusion **47** (2005) B263
- [4] M. Ono, S. M. Kaye, Y. -K. M. Peng, *et al.*, Nucl. Fusion **40**, 557 (2000)
- [5] T. K. Mau, S. C. Jardin, C. E. Kessel, *et al.*, Proceedings of the 18th IEEE/NPSS Symp. on Fusion Engineering, (Albuquerque, NM) 1999
- [6] D. A. Gates, R. Maingi, J. Menard, S. Kaye, S. A. Sabbagh, *et al.*, Physics of Plasmas **13**, (2006) 056122
- [7] S. Kaye, M. G. Bell, R. E. Bell, *et al.*, Nucl. Fusion **45** (2005) S168.
- [8] D. A. Gates, C. Kessel, J. Menard, G. Taylor, J.R. Wilson, *et al.*, Nucl. Fusion **46** (2006) S22
- [9] D. A. Gates, and the NSTX National Research Team, Phys. Plasmas **10** (2003) 1659
- [10] D. A. Gates, D. Mueller, C. Neumeyer, J. R. Ferron, IEEE Trans. on Nucl. Sci. **47** (2000) 222 (I)
- [11] D. A. Gates, J.R. Ferron, M. Bell, T. Gibney, R. Johnson, *et al.*, Fus. Eng. and Design **81** (2006) 1911
- [12] D.A. Gates, J.R. Ferron, M. Bell, T. Gibney, R. Johnson, *et al.*, Nucl. Fusion **46** (2006) 17
- [13] J. R. Ferron, M. L. Walker, L. L. Lao, H. E. St. John, D. A. Humphreys, J. A. Leuer, Nucl. Fusion **38** (1998) 1055
- [14] D. A. Gates, J. E. Menard, and R. J. Marsala, Rev. Sci. Inst. **75** (2004) 5090
- [15] S. A. Sabbagh, R. E. Bell, J. E. Menard, D. A. Gates, A. C. Sontag, *et al.*, Phys. Rev. Letters **97** (2006) 045004
- [16] J. E. Menard, *et al.*, *in these proceedings* Paper OV/2-4
- [17] F. Hofmann, J. M. Moret, D. J. Ward, Nucl. Fusion **38** (1998) 1767
- [18] A. Sykes, Plas. Phys. and Controll. Fusion **36** (1994) B93
- [19] R.J. Hawryluk, in Physics of Plasmas Close to Thermonuclear Conditions **1** 19 (CEC, Brussels, 1980)
- [20] O. Sauter, C. Angioni, and Y. R. Lin-Liu, Phys. Plasmas **6** (1999) 2834
- [21] J. E. Menard, R. E. Bell, D. A. Gates, S. M. Kaye, B. P. LeBlanc, *et al.*, Phys. Rev. Lett., **97** (2006) 095002
- [22] D.R. Mikkelsen, Physics of Fluids B **1** (1989) 333
- [23] T. M. Biewer, R. E. Bell, S. J. Diem, C. K. Phillips, J. R. Wilson, P. M. Ryan, Phys. Plasmas **12** (2005) 056108
- [24] R. W. Harvey, *et al.*, *in these proceeding* Paper No. TH/P6-11
- [25] J. R. Wilson, private communication
- [26] R. Maingi, M. G. Bell, R. E. Bell, *et al.*, Nucl. Fusion **43** (2003) 969
- [27] R. Maingi, K. Tritz, E. D. Fredrickson, *et al.*, Nucl. Fusion **45** (2005) 264
- [28] R. Majeski, *et al.*, *in these proceedings* Paper No. EX/P4-23